Room temperature ferromagnetism in ZnO prepared by microemulsion

Qingyu Xu,[1,a] Zheng Wen,[2] Hua Zhang,[1] Xiaosi Qi,[3] Wei Zhong,[3] Liguo Xu,[4] Di Wu,[2] Kai Shen,[4] and Mingxiang Xu[1]
[1]*Department of Physics, Southeast University, Nanjing 211189, China*
[2]*Department of Materials Science and Engineering, Nanjing University, Nanjing 210008, China*
[3]*Department of Physics, Nanjing University, Nanjing 210008, China*
[4]*School of Materials Science and Technology, Nanjing University of aeronautics and Astronautics, Nanjing 210016, China*

(Received 31 May 2011; accepted 21 July 2011; published online 2 August 2011)

Clear room temperature ferromagnetism has been observed in ZnO powders prepared by microemulsion. The O vacancy (V_O) clusters mediated by the V_O with one electron (F center) contributed to the ferromagnetism, while the isolated F centers contributed to the low temperature paramagnetism. Annealing in H_2 incorporated interstitial H (H_i) in ZnO, and removed the isolated F centers, leading to the suppression of the paramagnetism. The ferromagnetism has been considered to originate from the V_O clusters mediated by the H_i, leading to the enhancement of the coercivity. The ferromagnetism disappeared after annealing in air due to the reduction of H_i. [doi:10.1063/1.3624926]

Room temperature ferromagnetism has been observed in the traditionally nonmagnetic semiconductor oxide nanoparticles and films, such as ZnO, CeO_2, Al_2O_3, In_2O_3, HfO_2, and SnO_2, etc., and the defects have generally been considered to be the origin.[1–8] ZnO is a wide band gap semiconductor ($E_g \sim 3.3$ eV at 300 K) and has a large exciton binding energy (~ 60 meV), which has wide applications in optoelectronics.[9] ZnO has also attracted many research interests in its magnetic properties since the theoretical predication of the room temperature ferromagnetism in magnetic ion doped ZnO.[10] However, the defects responsible for the observed ferromagnetism in nondoped ZnO are still under debate. Zn defects,[3–5] O vacancies,[6,7] and Zn nanoclusters embedded in ZnO matrix,[8] have been considered to be the possible origin. Theoretically, O interstitial, Zn vacancy and O vacancy (V_O) clusters have been suggested to induce the ferromagnetism in ZnO.[6,11,12] Microemulsion is a low temperature synthetic method which might induce high concentration of defects. In this paper, we prepared ZnO powders by microemulsion. The magnetic properties and structure of the ZnO powders annealed in H_2 and air have been studied to clarify the magnetic contributions of the defects.

We followed A. Ishizumi's microemulsion method to prepare the ZnO powders.[13] We prepared two identical mixtures of octane, cetyl trimethyl ammonium bromide (CTAB), and butanol. An aqueous solution of Zn was added to one mixture, while aqueous ammonia was added to the other mixture. We then obtained two microemulsions with the aqueous solution encapsulated within the reverse micelles formed by surfactant (CTAB) and cosurfactant (butanol) in oil (octane): one contained Zn^{2+} ions, and the other contained OH^- ions. After mixing the two microemulsions, nanoparticles of hydroxide of Zn were yielded and were precipitated. The hydroxide nanoparticles were extracted from solution by a centrifugation and by a stir with ultrasound in de-ionized water. The nanoparticles of hydroxides were oxidized by heating at 100 °C for 60 min and were converted

[a]Corresponding author: xuqingyu@seu.edu.cn

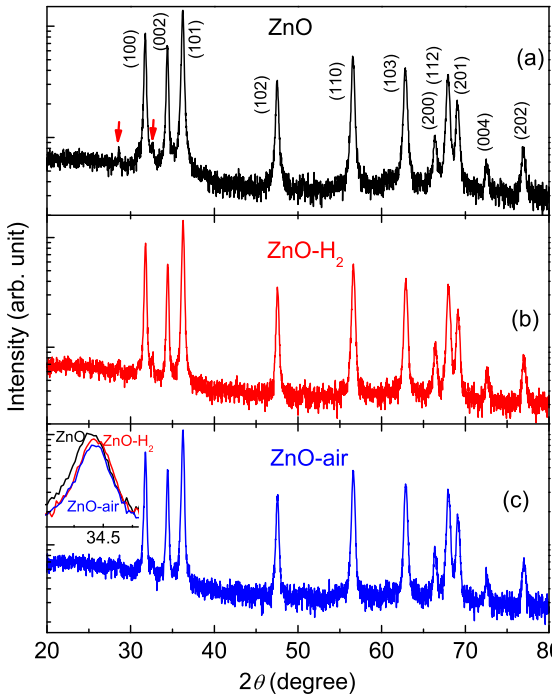

FIG. 1. XRD patterns of ZnO nanopowders, (a) as prepared, (b) annealed in H_2 at 500 °C for 2 h, (c) annealed in air at 500 °C for 2 h. The arrows mark the diffractions due to Cu K_β.

to ZnO nanocrystals (ZnO). The annealing of ZnO powders were performed in H_2 flow at 500 °C for 2 h (ZnO-H_2) and then annealed in air at 500 °C for another 2 h (ZnO-air). The structure was studied by X-ray diffraction (XRD) measurements with θ-2θ scans using a Cu $K\alpha$ source, transmission electron microscope (TEM, FEI Techni-S20), and X-ray photoelectron spectroscopy (XPS, ThermoFisher SCIENTIFIC) with Al Kα X-ray source ($h\nu$=1486.6 eV). The samples for XPS measurements were kept in the high-vacuum chamber overnight to remove the absorbed air. The Photoluminescence (PL) spectra of the samples were acquired at room temperature with acquisition time of 0.1 s by excitation with the 500 nm line of a Xe lamp (Horiba Jobin Yvon Fluorolog-3). The magnetization has been measured by a physical property measurement system (PPMS-9, Quantum Design) from 5 K to 300 K.

Figure 1 shows the XRD patterns of ZnO powders. The as-prepared and annealed ZnO powders all show the pure wurtzite structure without any impurity phases. To see the structural evolution of ZnO powders on the annealing, the (002) peaks of the samples are displayed in the inset of Fig. 1(c). It can be seen that the peaks shift to the higher angle for ZnO-H_2 and ZnO-air, indicating the decrease of the c lattice constant. This can be attributed to the decrease of V_O by annealing in H_2 and air.[7] Using the Debye-Scherrer equation D=0.9$\lambda/\beta\cos\theta$, where λ is the wavelength of the X-ray radiation, β the full width at half maximum (FWHM) of the diffraction peak and θ the scattering angle ((002) here),[14] the crystallite size of ZnO, ZnO-H_2 and ZnO-air is 33 nm, 32 nm and 32 nm, respectively. This shows that the grains didn't grow under the annealing temperature of 500 °C. Figure 2 shows the TEM images of ZnO and ZnO-H_2. Both the samples show the spindle shape with particle size of about 1 μm.

Figure 3(a) shows the *M-H* curves of the as-prepared ZnO powders. Hysteresis loop can be clearly observed at low fields indicating the ferromagnetism. The negative slope at high fields at 300 K indicates the diamagnetism from bulk ZnO, and changes to positive slope at 5 K indicating the existence of paramagnetism. The inset of Fig. 3(b) shows the room temperature PL spectra of ZnO powder. The strong green emission peak can be attributed to the oxygen vacancies.[15] As Banerjee suggested, this ferromagnetism can be explained by the V_O clusters mediated by the V_O with one

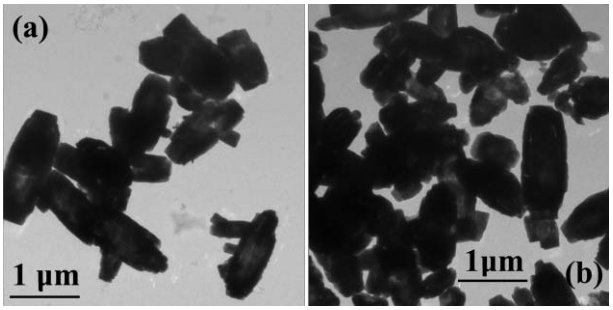

FIG. 2. Bright field TEM images of ZnO powders, (a) as-prepared and (b) annealed in H_2 at 500 °C for 2 h.

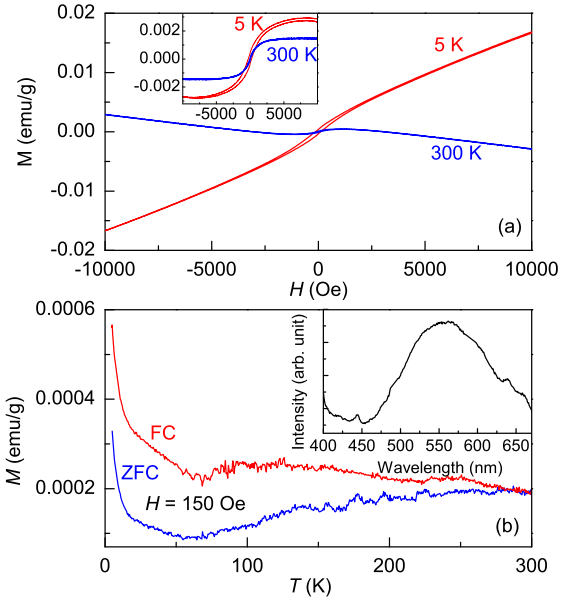

FIG. 3. (a) *M-H* curves of ZnO at 5 K and 300 K, the inset shows the enlarged view of *M-H* curves. (b) The ZFC and FC *M-T* curves of ZnO, the inset shows the PL spectrum.

electron (F center).[6,16] After subtracting the high field linear part, the ferromagnetic contributions at 5 K and 300 K are shown in the inset of Fig. 3(a). The saturate magnetization of 2.8×10^{-3} emu/g at 5 K and 1.5×10^{-3} emu/g at 300 K are in the range of the previous reported ferromagnetism in nonmagnetic semiconductors ($10^{-4}\sim10^{-3}$ emu/g).[1,6] Fig. 3(b) shows the field cooled (FC) and zero field cooled (ZFC) *M-T* curves measured under the field of 150 Oe. The distinct bifurcation can be observed below 300 K. The continuous increase of ZFC magnetization above 60 K with increasing temperature indicates the blocking moments. The sharp increase in the magnetization in both ZFC and FC curves below 60 K indicates the strong paramagnetic contribution from the isolated F centers.[6,16]

After annealing in H_2, the ferromagnetic magnetization is almost unchanged but the coercivity is much larger, as can be seen in Fig. 4(b). The slope of *M-H* curve at 5 K at high fields of ZnO-H_2 changes to negative (Fig. 4(a)), indicating that the paramagnetism from the isolated F centers disappeared after annealing in H_2. After annealing in air, the ferromagnetism disappeared, and only diamagnetism has been observed at 300 K (Fig. 4(b)).

The XPS survey spectra of the samples were taken (not shown here), and no impurities can be observed, indicating that the observed ferromagnetism is not from other ferromagnetic impurities. All the XPS spectra were referenced to the surface impurity C 1s line (284.8 eV) binding energy. Figure 5(a)–5(c) show the O 1s peaks. Double peaks have been applied to fit these peaks. The

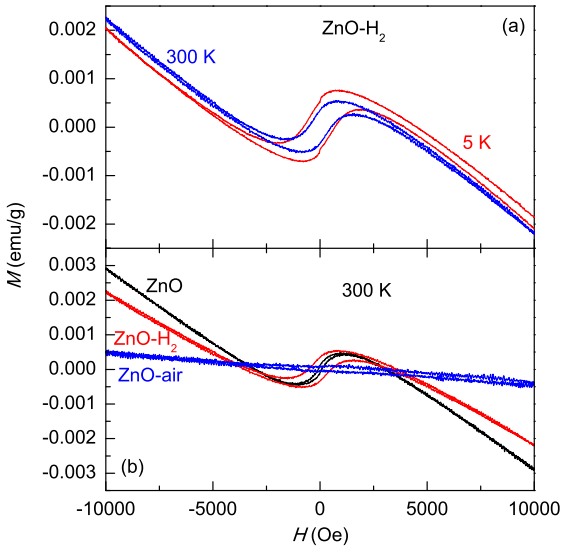

FIG. 4. (a) *M-H* curves for ZnO-H_2 at 5 K and 300 K. (b) *M-H* curves for ZnO, ZnO-H_2 and ZnO-air at 300 K.

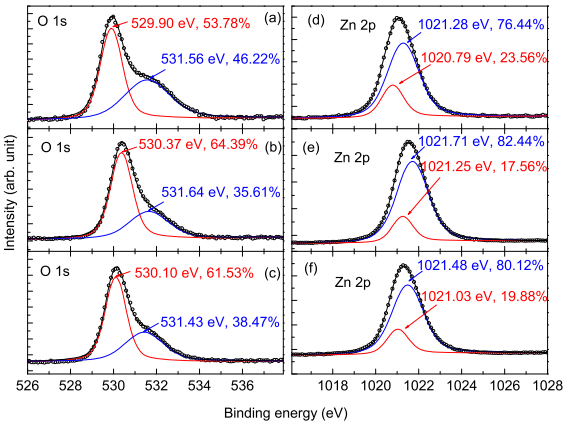

FIG. 5. XPS of O 1s for (a) ZnO, (b) ZnO-H_2, and (c) ZnO-air, and Zn 2p for (d) ZnO, (e) ZnO-H_2, and (f) ZnO-air. The fitted peak position and relative atomic concentration are indicated.

lower binding energy component (denoted as O_A) is corresponding to the stoichiometrically bonded O^{2-}, and the higher binding energy component (denoted as O_B) is attributed to the O^{2-} ions in the O deficient regions within the matrix of ZnO.[17,18] As can be seen, annealing in H_2 and air both decrease the concentration of O deficient region significantly. Since the ferromagnetic magnetization from V_O clusters was almost unchanged, and only isolated F center has magnetic moment of 1 μ_B,[6,16] we can conclude that the annealing in H_2 will effectively remove the isolated F centers. The asymmetric Zn 2p peaks can also be fitted by two peaks, the stoichometrically bonded Zn (higher binding energy, denoted as Zn_A), and the Zn in O deficient region (lower binding energy, denoted as Zn_B), as shown in Fig. 5(d)–5(f). Similar to O, the annealing in H_2 and air both decrease the concentration of Zn in the O deficient region.

Annealing in H_2 will incorporate H atoms into ZnO and locate at the interstitial sites as H_i or form V_O-H complex.[19] Considering the electron negativity of Zn (1.65) and H (2.20),[20] the peak positions of Zn and O shift to higher energy which can be assigned to H bonding.[21] Considering H_i and V_O-H, the nearest neighbor of H in stoichiometric region are O_A and Zn_A, while in O deficient region is Zn_B but little influence on O_B. Taken into account of the energy resolution of 0.1 eV, the peak positions of O_B for ZnO, ZnO-H_2 and ZnO-air are almost the same. The O_A, Zn_A and Zn_B peaks

all appear at higher energy than those of ZnO, confirming the incorporation of H after annealing in H_2. J. J. Dong reported that the V_O-H is quite stable while H_i diffuses out in ZnO after annealing in air at 500 °C.[19] However, the O_A, Zn_A and Zn_B peaks of ZnO-air all appear between those of ZnO and ZnO-H_2, indicating the both decrease of H_i and V_O-H after annealing in air.

Based on the XPS results, we can explain the observed magnetic properties of ZnO under different annealing conditions as following. In the as-prepared ZnO powder, the ferromagnetism comes from the V_O clusters mediated by the F centers and the paramagnetism comes from the isolated F centers.[6,16] After annealing in H_2, the isolated F centers were removed. The V_O clusters might be mediated by H_i instead of the F centers,[22] leading to the possible different magnetic anisotropy and thus the increase of the coercivity. After annealing in air, though there are still H_i, the concentration is much reduced, which cannot mediate the V_O clusters to form enough overlapped bound magnetic polarons,[23] leading to the disappearance of the ferromagnetism.

In summary, clear room temperature ferromagnetism and low temperature paramagnetism have been observed in ZnO powders prepared by microemulsion. The ferromagnetism originated from the F centers mediated O vacancy clusters, while the isolated F centers contributed to the low temperature paramagnetism. The XPS results confirmed the incorporation of interstitial H after annealing in H_2 at 500 °C. The isolated F centers have been removed, leading to the suppression of low temperature paramagnetism. The ferromagnetism has been concluded to originate from the O vacancy clusters mediated by the interstitial H, leading to the enhanced coercivity. This work clearly demonstrated that the ferromagnetism in ZnO might be mediated by the interstitial H, which will shed light on the development of ZnO-based spintronics devices.

ACKNOWLEDGEMENT

This work is supported by the National Natural Science Foundation of China (50802041, 50872050), National Key Projects for Basic Researches of China (2009CB929503, 2010CB923404), NCET-09-0296 and Southeast University. M. X. Xu acknowledges the support from the National Science Foundation of Jiangsu Province of China (Grant No. BK2010421).

[1] A. Sundaresan, R. Bhargavi, N. Rangarajan, U. Siddesh, and C. N. R. Rao, Phys. Rev. B **74**, 161306(R) (2006).
[2] E. Tirosh and G. Markovich, Adv. Mater. **19**, 2608 (2007).
[3] N. H. Hong, J. Sakai, and V. Brizé, J. Phys.: Condens. Mater. **19**, 036219 (2007).
[4] Q. Xu, H. Schmidt, S. Zhou, K. Potzger, M. Helm, H. Hochmuth, M. Lorenz, A. Setzer, P. Esquinazi, C. Meinecke, and M. Grundmann, Appl. Phys. Lett. **92**, 082508 (2008).
[5] M. Khalid, M. Ziese, A. Setzer, P. Esquinazi, M. Lorenz, H. Hochmuth, M. Grundmann, D. Spemann, T. Butz, G. Brauer, W. Anwand, G. Fischer, W. A. Adeagbo, W. Hergert, and A. Ernst, Phys. Rev. B **80**, 035331 (2009).
[6] S. Banerjee, M. Mandal, N. Gayathri, and M. Sardar, Appl. Phys. Lett. **91**, 182501 (2007).
[7] B. Panigraphy, M. Aslam, and D. Bahadur, Appl. Phys. Lett. **98**, 183109 (2011).
[8] J. B. Yi, H. Pan, J. Y. Lin, J. Ding, Y. P. Feng, S. Thongmee, T. Liu, H. Gong, and L. Wang, Adv. Mater. **20**, 1170 (2008).
[9] Ü. Özgür, Ya. I. Alivov, C. Liu, A. Teke, M. A. Reshchikov, S. Doğan, V. Avrutin, S.–J, Cho, and H. Morkoç, J. Appl. Phys. **98**, 041301 (2005).
[10] T. Dietl, H. Ohno, F. Matsukura, J. Cibert, and D. Ferrand, Science **287**, 1019 (2000).
[11] X. Zuo, S. Yoon, A. Yang, W. Duan, C. Vittoria, and V. G. Harris, J. Appl. Phys. **105**, 07C508 (2009).
[12] Q. Wang, Q. Sun, G. Chen, Y. Kawazoe, and P. Jena, Phys. Rev. B **77**, 205411 (2008).
[13] A. Ishizumi and Y. Kanemitsu, Appl. Phys. Lett. **86**, 253106 (2005).
[14] A. Jagannatha Reddy, M. K. Kokila, H. nagabhushana, R. P. S. Chakradhar, C. Shivakumara, J. L. Rao, and B. M. Nagabhushana, J. Alloys Compd. **509**, 5349 (2011).
[15] Y. F. Mei, G. G. Siu, R. Y. Fu, P. Chu, Z. M. Li, and Z. K. Tang, Appl. Surf. Sci. **252**, 2973 (2006).
[16] J. M. D. Coey, A. P. Douvalis, C. B. Fitzgerald, and M. Venkatesan, Appl. Phys. Lett. **84**, 1332 (2004).
[17] H. Tong, Z. Deng, Z. Liu, C. Huang, J. Huang, H. Lan, C. Wang, and Y. Cao, Appl. Surf. Sci. **257**, 4906 (2011).
[18] D. Elizabeth Pugel, R. D. Vispute, S. S. Hullavarad, T. Venkatesan, and B. Varughese, Appl. Surf. Sci. **254**, 2220 (2008).
[19] J. J. Dong, X. W. Zhang, J. B. You, P. F. Cai, Z. G. Yin, Q. An, X. B. Ma, P. Jin, Z. G. Wang, and P. Chu, ACS Appl. Mater. Interfaces **2**, 1780 (2010).
[20] http://www.webelements.com/
[21] R. K. Singhal, S. Kumar, Y. T. Xing, U. P. Deshpande, T. Shripathi, S. N. Dolia, and E. Saitovitch, Mater. Lett. **65**, 1485 (2011).
[22] W. Hao, J. Li, H. Xu, J. Wang, and T. Wang, ACS Appl. Mater. Interfaces **2**, 2053 (2010).
[23] J. M. D. Coey, M. Venkatesan, and C. B. Fitzgerald, Nature Mater. **4**, 173 (2005).